FEBS Letters 575 (2004) 14–18 FEBS 28773

Phenotypic selection and characterization of randomly produced non-haemolytic mutants of the toxic sea anemone protein sticholysin II

Jorge Alegre-Cebollada[a], Valle Lacadena[a], Mercedes Oñaderra[a], José M. Mancheño[b], José G. Gavilanes[a], Álvaro Martínez del Pozo[a,*]

[a] *Facultad de Química, Departamento de Bioquímica y Biología Molecular, Universidad Complutense, 28040 Madrid, Spain*
[b] *Grupo de Cristalografía, Instituto de Química-Física Rocasolano, CSIC, Serrano 199, 28006 Madrid, Spain*

Received 29 June 2004; revised 9 August 2004; accepted 14 August 2004

Available online 26 August 2004

Edited by Peter Brzezinski

Abstract A rapid screening method for haemolytic activity, using blood agar plates, has been developed to analyze randomly produced mutant variants of the pore-forming protein sticholysin II (Stn II). Those exhibiting a reduced activity were selected and the DNA corresponding to each Stn II variant sequenced. Once the mutation produced was determined, protein variants were isolated and characterized in terms of structure (circular dichroism spectra and thermal stability) and haemolytic activity. Three single mutation protein variants, at residues K19, F106 and Y111, showed a significantly decreased haemolytic activity while their thermostability was identical to that of the wild-type protein. Considering the obtained data and based on the three-dimensional structure of the protein, the role of these residues on the mechanism of haemolysis has been analyzed.

Keywords: Actinoporin; Equinatoxin; Haemolysis screening; Random mutation; Protein structure

1. Introduction

Actinoporins are a family of 20 kDa pore-forming proteins produced by sea anemones displaying 65–85% sequence similarity [1]. These cysteineless and basic proteins, highly soluble in aqueous solvents, oligomerize to form cation-selective pores in the presence of some phospholipid membranes [2,3], which are responsible for their cytolytic effect on erythrocytes, platelets, and fibroblasts [1]. The three-dimensional structures of two actinoporins, equinatoxin II (Eqt II) from *Actinia equina* and sticholysin II (Stn II) from *Stichodactyla helianthus*, have been solved [4–6]. Both proteins display a very similar β-sandwich fold composed of 10 β-strands flanked on each side by two short α-helices (Fig. 1A). The structure of a complex between monomeric Stn II and phosphocholine (POC) has also been determined [6], revealing the existence of a putative phospholipid-binding site (Fig. 1B). In contrast to other pore-forming proteins, the mechanism of actinoporin pore formation is poorly defined in spite of the models derived from the structural data [4–6]. Elucidation of specific protein residues involved in the lytic action will improve the knowledge about these proteins synthesized as water-soluble monomers but able to form oligomeric pores within membranes. Based on this idea, we have randomly produced mutants of Stn II in order to select those with diminished haemolytic activity. We have developed a fast screening method useful to select those mutants with an altered ability to lyse erythrocytes. The role of the mutated residues has been discussed in terms of structure–function relationships of this protein.

2. Materials and methods

2.1. Production of the mutants

A 6His-tagged version of Stn II has been overproduced in *Escherichia coli* RB791 cells and purified to homogeneity [7]. The same plasmid and strategy were used to produce and purify the mutants selected. Recombinant DNA methods other than those reported below were performed according to standard procedures [8]. Diversify PCR Random Mutagenesis Kit (Clontech) was used to carry out controlled random mutagenesis using the original plasmid as template where Stn II was cloned (pQE306HStnII) [7]. Considering the Stn II-coding cDNA size (~550 bp) and following the manual instructions, a concentration of 0.2 mM Mg^{2+} was employed. In these conditions, the mutation rate should be around 2 mutations per 1000 bp. This low mutation rate was employed in order to minimize the introduction of multiple changes within the same Stn II-coding cDNA molecule. The amplified pool of DNA molecules was isolated, digested with *Bam*HI and *Hin*dIII, cloned again in pQE30 and used to transform *E. coli* RB791 cells. In order to screen for their haemolytic activity, single colonies were grown in 5 ml of LB at 37 °C up to an OD_{600} of 1.0. Then, IPTG was added to 2.0 mM final concentration and the cells were further incubated for 4 h. After this time, the cells were pelleted, resuspended in 1.0 ml of water, and disrupted by ultrasonication. The suspension was centrifuged at 14 000×*g* for 10 min at 4 °C. Supernatants were heated at 53 °C for 10 min. Wild-type Stn II is a rather thermostable protein [9] that remains fully haemolytic after this treatment.

2.2. Haemolytic screening of the mutants

The haemolytic activity of the above solutions was analyzed in sheep blood agar plates (Dismalab, Spain) by adding from 1:1 to 1:5 dilutions of them, followed by an overnight incubation at 37 °C. Omission of the above heating step at 53 °C resulted in growth of bacteria, preventing the correct interpretation of the results. The haemolytic fractions produced clear halos. This procedure is sensitive enough to detect a haemolytic activity equivalent to that of 0.2 ng of Stn II. The supernatants and resuspended pellets from colonies corresponding to smaller or low-clarity halos were analyzed by means of 0.1% SDS–15% PAGE, performed according to standard procedures [7], to identify those that still produced enough of the recombinant protein. Those

* Corresponding author. Fax: +34-913944159.
E-mail address: alvaro@solea.quim.ucm.es (Á. Martínez del Pozo).

Abbreviations: Eqt II, equinatoxin II; POC, phosphocholine; Stn II, sticholysin II

0014-5793/$22.00
doi:10.1016/j.febslet.2004.08.031

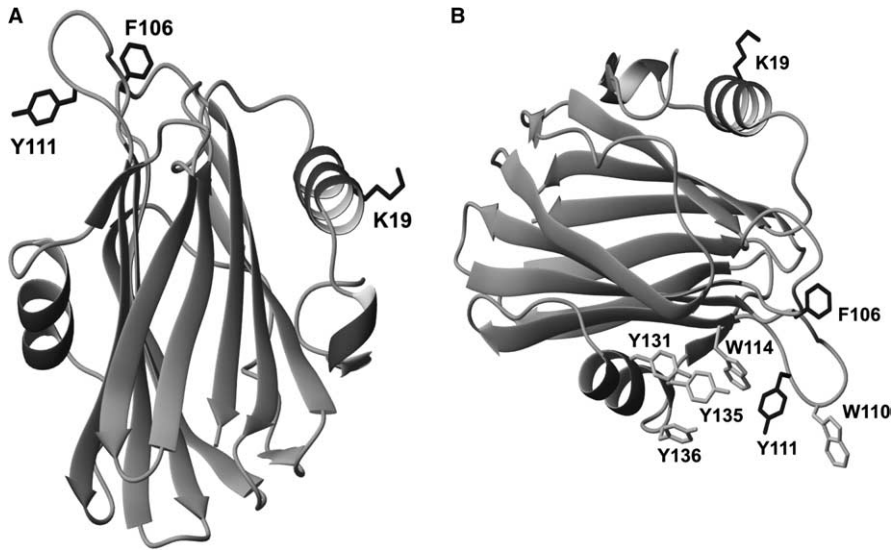

Fig. 1. (A) Diagram of the three-dimensional structure of Stn II (Protein Data Bank accession number 1GWY) where three of the residues mentioned in the text are highlighted, Lys-19, Phe-106 and Tyr-111. (B) Diagram of the 3D-structure of Stn II where the aromatic residues involved in the POC-binding site of the protein (in grey) are shown as well as Lys-19, Phe-106 and Tyr-111 (in black). Tyr-111 is part of the cluster of aromatic residues involved in the POC-binding site [6]. Diagrams were generated with MOLMOL [15] and subsequently rendered with MegaPov.

colonies were streaked on LB-Amp plates and used to purify the corresponding plasmid, using the GeneElute Miniprep Kit system from Sigma. Finally, these DNA were sequenced at the DNA Sequencing Facility of the Complutense University in order to identify the mutation presumably responsible for this lack of haemolytic activity.

2.3. Proteins purification

The *E. coli* colonies containing the mutants selected were grown in one liter of LB-Amp and protein production was induced with IPTG, as described above. The mutant proteins were purified as reported before [7] for the wild-type protein. Essentially, the supernatant resulting from the sonication of the cells was loaded onto a Ni^{2+}–nitrilotriacetic acid agarose (Ni–NTA) and eluted with 10 mM Mops buffer, pH 8.0, containing 250 mM imidazole, after performing washing steps with lower concentrations of imidazole [7]. Analysis of total protein produced by the different bacterial colonies assayed as well as homogeneity of the purified proteins was performed by 0.1% SDS–15% polyacrylamide gel electrophoresis.

2.4. Haemolytic assays

Haemolytic assays using sheep erythrocytes were performed as described before [7,10]. Erythrocytes from heparinized sheep blood (Dismalab, Spain) were washed and resuspended in 10 mM Tris–HCl, pH 7.4, containing 0.145 M NaCl, to a final concentration that resulted in an OD_{540} of 0.7 when completely lysed by mixing 100 μl of the cell suspension with 750 μl of 0.1% Na_2CO_3 (p/v). The standard haemolytic assay was performed by adding increasing concentrations of protein to 400 μl aliquots of the erythrocytes suspension, previously 4-fold diluted with the same buffer. This reaction mixture was incubated for 30 min at 37 °C, with gentle shaking to avoid sedimentation of the cells. Then, the tubes were microfuged and the absorbance values at 540 of the supernatants were measured in a spectrophotometer. The percentage of haemolysis was calculated from the absorbance values by comparison with that obtained after lysing the cells with 0.1% Na_2CO_3 (p/v) as 100%. The HC_{50} (protein concentration required to produce 50% haemolysis) was calculated from percentage of haemolysis versus protein concentration plots.

2.5. Spectroscopic characterization

Protein solutions were prepared in 15 mM Mops buffer, pH 7.5, containing 0.1 M NaCl at concentrations ranging from 0.2 to 1.0 mg/ml depending on the spectroscopy used. Absorbance measurements were carried out on an Uvikon 930 spectrophotometer at 100 nm/min scanning speed, at room temperature, and in 1-cm optical-path cells. Far-UV circular dichroism (CD) spectra were obtained on a Jasco 715 spectropolarimeter at 0.2 nm/second scanning speed in 0.1-cm optical-path cells. Each final spectrum was the average accumulation of at least four scans. Mean residue weight ellipticities were expressed in units of degree cm^2 $dmol^{-1}$. At neutral pH, Stn II is an associating monomer–tetramer system with an association constant of 10^9 M^{-3} [11], and its thermal denaturation occurs with a fast aggregation in a concentration dependent process [9]. Thus, thermal denaturation profiles of the protein can be obtained by measuring the temperature dependence of either optical-path clarification (by CD measurements at 218 nm) or Rayleigh light scattering (by fluorescence measurements at 330 nm for excitation at the same wavelength) [9] in the range of 25–85 °C, the temperature being continuously changed at a rate of 0.5 °C/min. Results are expressed as percentages of the total spectroscopic variation versus temperature. The T_m value was considered as the temperature at the midpoint of the monophasic thermal transitions observed.

3. Results and discussion

We have standardized an easy procedure for the screening of haemolytic activity of Stn II in sheep blood agar plates that produces reliable data (Fig. 2). Seventy-three different *E. coli* colonies transformed with a pool of randomly mutated molecules of the pQE306HStnII plasmid were assayed for haemolysis on these blood agar plates. Only 22 of them proved non-haemolytic. Small-scale production experiments revealed that 15 out of these 22 colonies produced significant amounts of a protein of the same molecular mass as wild-type Stn II, according to their electrophoretic behaviour in SDS–PAGE. Plasmids from these 15 colonies were isolated and the DNA corresponding to each Stn II variant was completely sequenced. The mutations found are shown in Table 1.

Five of these colonies harboured mutated plasmids that resulted in the production of an insoluble protein variant. Therefore, these mutations impair the proper folding of the proteins, which would explain their lack of solubility. Two of them corresponded to the Trp-43 residue (W43R), two others contained a double mutation (N65Y/F102L and F102L/

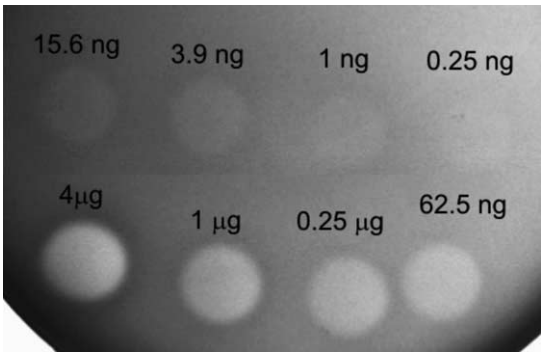

Fig. 2. Haemolytic assay on blood-agar plates. Different amounts of Stn II, dissolved in PBS, previously heated at 53 °C for 10 min and ranging from 4 μg to 0.25 ng were assayed. The clear halos correspond to the haemolytic activity of the protein.

Table 1
Amino acid changes in Stn II deduced from the mutations detected in the corresponding plasmids isolated from non-haemolytic colonies of transformed *E. coli* RB791 cells that produced significant amounts of the protein

Mutation[a]
F14Y (+)
K19E (+)
N37S (−)
W43R[b] (−)
N65Y/F102L (−)
K67E (+)
F102L (+)
T97A/K118R (+)
N96D/Y135N (+)
F102L/G152E (−)
G95E/W146G (+)
F106L (+)
Y111N (+)
N144S (+)

[a] Amino acid numeration is given according to the sequence of the wild-type protein produced by the anemone *Stichodactyla helianthus*.
[b] This mutation was found twice; (+) the protein remains soluble after ultrasonication or (−) appears in the insoluble pellet.

G152E), and the fifth one was N37S (Table 1). Most of these residues (Asn65 was the only exception) are located in β-strands. Trp-43 is buried in the hydrophobic core of the protein (Fig. 3A). Asn-37 is involved in two hydrogen bonds that would maintain the loop between β2 and β3 strands (Fig. 3A). Mutation of Phe-102 resulted in a dramatic decrease of the protein stability (Table 2; see below), which when combined with a second mutation would explain the insolubility of N65Y/F102L and F102L/G152E. Three more mutants were soluble but also contained a double mutation that would make it difficult to unambiguously assign the effects observed.

The seven remaining mutant variants were produced and purified to homogeneity. Their far-UV CD spectra (Fig. 4A) were indistinguishable from that of the wild-type protein, indicating that the active three-dimensional conformation of Stn II was preserved. However, large differences were observed in terms of their haemolytic activity against sheep erythrocytes suspensions. As it can be observed in Table 2, two groups of proteins could be distinguished. The first one displayed very similar HC_{50} values to the wild-type protein. However, these variants showed a dramatically decreased thermal stability (they showed a reduction in their T_m values ranging between 12 and 20 °C; Fig. 4B and Table 2), which would explain the reduced haemolytic activity on agar-blood plates of the producing colony. Therefore, these mutations (F14Y, K67E, F102L, and N144S) correspond to amino acid residues with a crucial role in the protein stability but not involved in the haemolytic mechanism. In fact, when these purified proteins were incubated for 10 min at a temperature of 53 °C, the corresponding HC_{50} values were 2–3-fold increased (for F102L no haemolytic activity was observed even at 20 nM protein concentration), while this treatment did not modify the haemolytic activity of the wild-type protein. Again, the localization of these mutations within the Stn II structure is in accordance with this idea. All of them are conserved in Eqt II and the first three are also located in elements of ordered secondary structure. Phe-14 is located in the N-terminal α-helix and shows van der Waals interactions (distance < 4.5 Å) with Ile-160, Thr-162 and methylene groups of Lys-168 (Fig. 3B). The one remaining, N144S, corresponds to a residue of the loop connecting the second α-helix and the β8 strand (Fig. 3B). It is close to Phe-14 and at hydrogen bond distance of Ser-163. Lys-67, although highly exposed, is a well ordered residue as deduced by the perfectly defined side chain electron density. This is probably due to the existence of van der Waals interactions (distance < 4.0 Å) with Pro-64 and Ala-8, which presumably maintains Lys-67 in a conformation adequate for hydrogen bond formation between the peptide NH group of Lys-67 and the CO group of Pro-64 that may be of critical function in maintaining the loop between β4 and β5 strands (Fig. 3C).

The other three mutant proteins remaining (K19E, F106L, and Y111N) showed a significantly decreased haemolytic activity while their thermostability was identical to that of the wild-type protein, at least in terms of their T_m values (Table 2). Close inspection of Stn II three-dimensional structure allows the discussion about the role of these residues on the mechanism of haemolysis.

As indicated before, the main core of the Stn II three-dimensional structure is a β-sandwich fold composed of 10 β-strands, flanked on each side by two short α-helices (Fig. 1A). These α-helices interact with the β-sandwich predominantly through hydrophobic interactions and van der Waals contacts, but salt bridges are also observed [6]. The current model accepted to explain the pore formation mechanism of actinoporins assumes that they must proceed through at least three steps: monomeric binding to the membrane interface, assembly of four monomers, and final formation of the functional pore. According to this model, the N-terminal region would be involved initially in oligomerization through interactions with the C-terminal region of the adjacent monomer [6]. Thus, the assembly of four monomers at the membrane interface would involve protein–protein interactions mediated by residues comprised within the first 29 amino acids stretch. Regarding the K19E mutant, this lysine residue is located within the helix α1 protruding out towards the solvent (Fig. 3D). Thus, it seems feasible to consider that this residue might participate in establishing interactions with the lipid interface and/or with an adjacent monomer during the formation of the pore complex. In this sense, according to the high resolution model of the tetrameric assembly of Stn II, Lys-19 would be located in the close vicinity of the lipid interface [6], which makes the first possibility more plausible. Moreover, this hypothesis would be consistent with

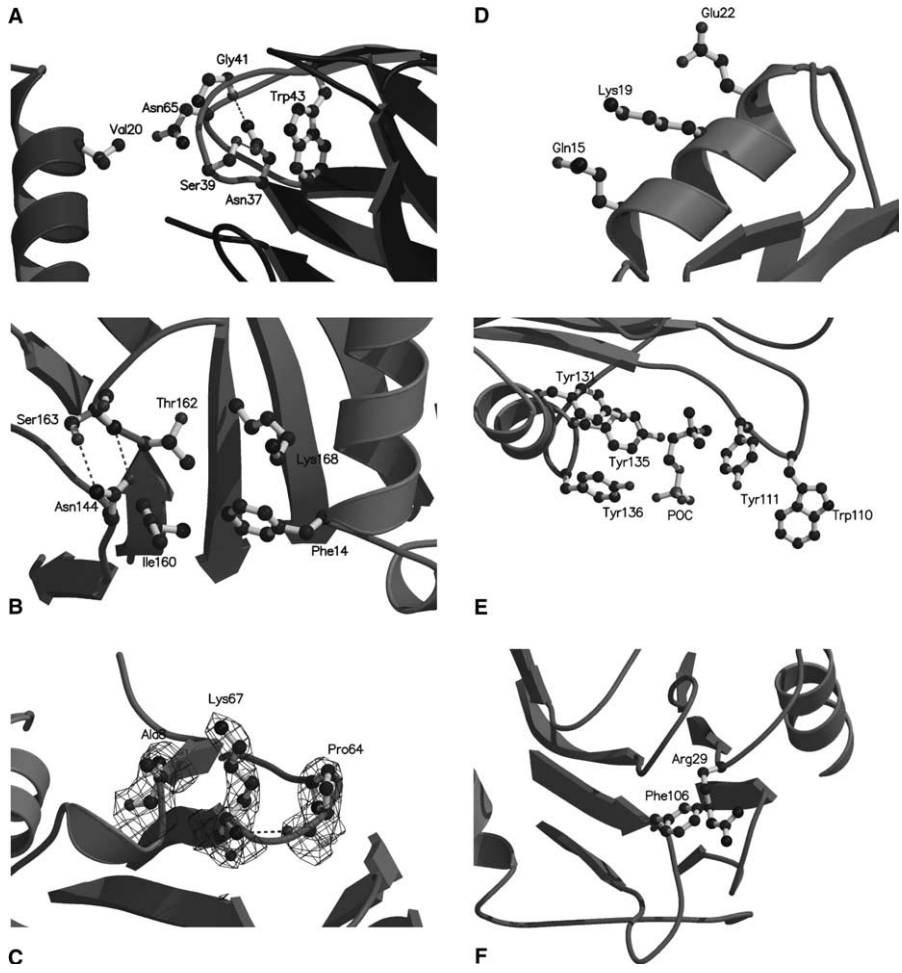

Fig. 3. Diagrams of detailed portions of the 3D-structure of Stn II (accession number 1GWY) corresponding to the environment of selected residues: (A) Asn-37, Trp-43 and Asn-65; (B) Phe-14 and Asn-144; (C) Lys-67; (D) Lys-19; (E) Tyr-111 (this picture is obtained from the crystal structure of Stn II-POC complex; Protein Data Bank accession number 1O72); (F) Phe-106. Diagrams were generated with MOLSCRIPT [16] and RASTER3D [17].

Table 2
Thermal stability and haemolytic activity parameters of wild-type Stn II and its non-haemolytic soluble mutant variants

Protein	T_m (°C)	ΔT_m (°C)[a]	HC_{50} (nM)	Relative HC_{50}[b]
Wild-type	67	–	0.55	1.00
F14Y	55	−12	0.42	0.76
K19E	65	−2	3.86	7.02
K67E	55	−12	0.64	1.16
F102L	47	−20	0.46	0.84
F106L	66	−1	2.17	3.95
Y111N	67	0	1.37	2.49
N144S	55	−12	0.55	1.00

[a] $\Delta T_m = T_m(\text{mutant}) - T_m(\text{wild-type})$.
[b] Relative $HC_{50} = HC_{50}(\text{mutant})/HC_{50}(\text{wild-type})$.

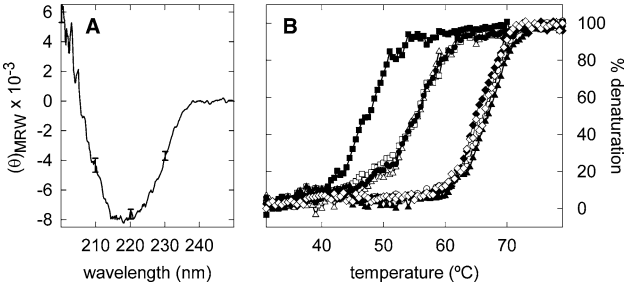

Fig. 4. (A) Far-UV circular dichroism spectrum of wild-type Stn II at neutral pH. Vertical bars at selected wavelengths show the ellipticity range where the spectra of the seven Stn II mutant variants purified are included. Mean residue weight ellipticity values $(\theta)_{MRW}$ are expressed in units of degree cm^2 $dmol^{-1}$ of amino acid residue. (B) Thermal denaturation profiles of: (○) wild-type Stn II; and mutant variants (▲) Y111N; (●) N144S; (Δ) K67E; (■) F102L; (□) F14Y; (◆) K19E; (◇) F106L. Values are expressed as percentages from CD measurements at 218 nm.

the existence of a threonine in Eqt II, as the presence of this residue near the lipid interface is energetically favourable [12]. If such is the case, the charge reversal produced by the K19E mutation would affect dramatically to the stabilization effect of this interaction with the lipid interface, thus rendering this Stn II variant as a less efficient haemolytic protein.

In order to explain the effect of the Y111N mutant it should be taken into account that, according to the mentioned model, the first step of the pore forming mechanism would be binding of Stn II monomers to the membrane interface. This step would be driven by binding of the POC moiety of some phospholipids to a specific location of the protein [6]. This location is a cavity where the positively charged choline is stabilized by cation-π interactions with the aromatic rings of Tyr-111 and Tyr-135 (Fig. 3E). Indeed, the phosphate moiety

of POC also interacts with the hydroxyl phenolic group of Tyr-111. Obviously, neither of the two interactions can be established for the Y111N variant of Stn II which can easily explain why this mutant is less haemolytic than the wild-type protein. This result also seems to confirm the role previously assigned to the Stn II POC binding site within the pore formation mechanism.

The third less haemolytic mutation selected was F106L. This Phe residue is located within the loop connecting strands β6 and β7 and quite close to the POC binding site in the three-dimensional structure of Stn II (Fig. 1B). It is part of an exposed cluster of aromatic amino acids which, at least in Eqt II, participate in membrane binding [13]. Considering these observations, as well as the fact that these aromatic residues have affinity for the membrane interface [14], it is reasonable to assume that a Leu residue could not play the role assigned to this Phe in this regard. In fact, comparison of the structures of free Stn II and that of the complex Stn II:POC revealed some backbone modifications in the mentioned loop between strands β6 and β7 [6], suggesting again that this protein region is involved in binding to the membrane. Thus, the behaviour of the F106L mutant would confirm both the role of the POC-binding site and the aromatic amino acids cluster in driving the binding of Stn II to the membranes. In addition, Phe-106 interacts with Arg-29 through cation-π interactions (Fig. 3F). Arg-29 is located in the loop after the N-terminal α-helix, which would act as a hinge region in the conformational change involved in the 3D-model of the pore-like structures of Stn II [6].

In summary, the method presented in this work to produce and isolate different mutant variants of Stn II has resulted to be useful in selecting significantly less haemolytic mutants which maintain their overall native conformation and thermostability. In addition, the analysis of the three protein variants containing the single mutations K19E, F106L, and Y111N has also been useful in order to discuss the role of specific regions of the protein in terms of structure–function relationships.

Acknowledgements: This research was supported by Grant BMC2003-03227 (MCYT, Spain).

References

[1] Maçek, P., Belmonte, G., Pederzolli, C. and Menestrina, G. (1994) Toxicology 87, 205–227.
[2] Martín-Benito, J., Gavilanes, F., de los Ríos, V., Mancheño, J.M., Fernández, J.J. and Gavilanes, J.G. (2000) Biophys. J. 78, 3186–3194.
[3] Anderluh, G. and Maçek, P. (2002) Toxicon 40, 111–124.
[4] Athanasiadis, A., Anderluh, G., Maçek, P. and Turk, D. (2001) Structure 9, 341–346.
[5] Hinds, M.G., Zhang, W., Anderluh, G., Hansen, P.E. and Norton, R.S. (2002) J. Mol. Biol. 315, 1219–1229.
[6] Mancheño, J.M., Martín-Benito, J., Martínez-Ripoll, M., Gavilanes, J.G. and Hermoso, J.A. (2003) Structure 11, 1319–1328.
[7] de los Ríos, V., Oñaderra, M., Martínez-Ruiz, A., Lacadena, J., Mancheño, J.M., Martínez del Pozo, A. and Gavilanes, J.G. (2000) Protein Exp. Purif. 18, 71–76.
[8] Sambrook, J. and Russell, D.W. (2001) Molecular Cloning. A Laboratory Manual, 3rd edn. Cold Spring Harbor Laboratory Press, Cold Spring Harbor.
[9] Mancheño, J.M., De Los Ríos, V., Martínez del Pozo, A., Lanio, M.E., Oñaderra, M. and Gavilanes, J.G. (2001) Biochim. Biophys. Acta 1545, 122–131.
[10] de los Ríos, V., Mancheño, J.M., Lanio, M.E., Oñaderra, M. and Gavilanes, J.G. (1998) Eur. J. Biochem. 252, 284–289.
[11] de los Ríos, V., Mancheño, J.M., Martínez del Pozo, A., Alfonso, C., Rivas, G., Oñaderra, M. and Gavilanes, J.G. (1999) FEBS Lett. 455, 27–30.
[12] Whimley, W.C. and White, S.H. (1996) Nat. Struct. Biol. 3, 842–848.
[13] Hong, Q., Gutiérrez-Aguirre, I., Barlic, A., Malovrh, P., Kristan, K., Podlesek, Z., Maçek, P., Turk, D., González-Mañas, J.M., Lakey, J.H. and Anderluh, G. (2002) J. Biol. Chem. 277, 41916–41924.
[14] Killian, J.A. and Von Heijne, G. (2000) Trends Biochem. Sci. 25, 429–434.
[15] Koradi, R., Billeter, M. and Wütrich, K. (1996) J. Mol. Graph. 14, 51–55.
[16] Kraulis, P.J. (1991) J. Appl. Crystallogr. 24, 946–950.
[17] Merrit, E.A. and Bacon, D.J. (1997) Methods Enzymol. 277, 505–524.